A VISCO-ELASTIC SANDWICH SOLUTION FOR ORTHOTROPIC DECKS OF STEEL BRIDGES

Ronaldo C. Battista*, Emerson F. dos Santos ** , Raimundo Vasconcelos *** and Michèle S. Pfeil*

* Instituto COPPE
e-mails: battista@coc.ufrj.br, mpfeil@coc.ufrj.br

** Petrobrás
e-mail: emersonfigueiredo@petrobras.com.br

** * Universidade Federal do Amazonas
e-mail: vasconcelos@ufam.edu.br

Keywords: steel bridges, orthotropic deck, vehicle–structure dynamic interaction, viscoelastic material.

Abstract. *This paper presents and discusses alternatives to enhance the fatigue performance of lightweight and slender steel decks of box-girders bridges. Solutions were devised by adding to the steel deck a reinforced concrete slab in two different manners: (i) a sandwich structure in which a visco-elastic layer is inserted in between the steel plate and the concrete slab and (ii) a composite deck formed by the same concrete slab fixed with stud connectors to the steel deck plate. The performances of these composite orthotropic decks of bridge structures undergoing the effects of the dynamic interaction between vehicles, pavement and the structure itself are assessed by means of a computational tool specially developed to this end. It is shown that the sandwich deck displays lower peak displacement and stresses amplitudes than the composite deck counterpart and therefore can be adopted as a rational solution in the design of new bridges and also be employed in the rehabilitation of slender orthotropic decks of existing steel bridges.*

1 INTRODUCTION

To investigate the structural behaviour of typical slender orthotropic steel decks under dynamic action of heavy trucks traveling with constant velocities on rough surface of asphalt pavements and also to investigate the performance of two devised composite structural solutions in attenuating displacements and stresses amplitudes it was used as a case study a stretch of the slender ortrotropic steel deck of the central span of Rio-Niterói bridge, which crosses the Guanabara Bay at Rio de Janeiro, Brazil.

Figures 1 refer to several details of the orthotropic deck of the steel twin-box-girders of the Rio-Niteroi highway bridge which, before its rehabilitation in 2001 used to be, under stochastic traffic loading, frequently damaged by fatigue cracks in the welded joints and geometric details [1,2,3]. Cracks were first and more frequently observed in the welded details illustrated in Figs. 1.b, 1.c and 1.d: (i) the longitudinal welded connection between the deck plate and rib web; (ii) the transversal field-butt-welded connections of ribs and the welded splice plates; (iii) the welded connections between the ribs and the trapezoidal shape splice plates, and between these and the floorbeam web.

To enhance the fatigue performance of this and other orthotropic steel deck solutions were devised [2,3,4] by adding to the steel deck a reinforced concrete slab in two different manners as shown in Figure 2: (i) a sandwich structure in which a visco-elastic layer was inserted in between the steel plate and the concrete slab and (ii) a composite deck formed by the same concrete slab fixed with stud connectors to the steel deck plate. These two alternatives were tested on a prototype scale model [3] constructed in the

Structures Laboratory of the Instituto COPPE/UFRJ (see Figure 3). While the composite deck displayed greater reductions in static stresses in relation to the unreinforced deck, the sandwich alternative showed greater modal damping factors.

Preliminary numerical studies served to show some important advantages of the sandwich alternative over the conventional counterpart. But because of the lack of technical understanding of the innovative sandwich solution and also because of the tight schedule to finish up the rehabilitation work the more conventional composite deck solution was adopted by the Rio-Niterói bridge administration. Experimental dynamic measurements for normal traffic loading on the composite deck made after its completion corroborated some important aspects of its structural behaviour which had been already pointed out in previous experimental and numerical studies [4].
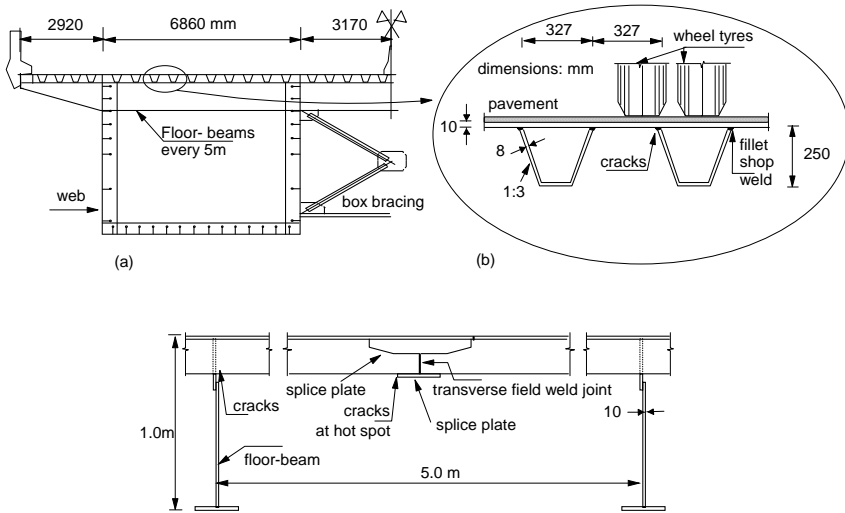
Figure 1: The orthotropic deck of the Rio-Niteroi bridge.
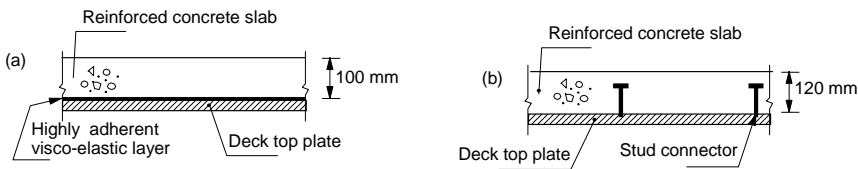
Figure 2: Alternative solutions to enhance the ultimate fatigue life of an orthotropic deck: (a) sandwich structure; (b) composite deck.

The performances of these composite orthotropic decks of bridge structures undergoing the effects of the dynamic interaction between vehicles, pavement and the structure itself were later assessed by means of a computational tool specially developed to this end [5,6,7]. In this tool, called CONTROLMADS, several finite elements are available, including a hexahedral element to represent visco-elastic components.

This paper presents and discusses the most relevant points of these studies and the main numerical results obtained for the two orthotropic deck alternatives under the action of a 3 axles heavy truck traveling with constant velocities. It is shown that the sandwich deck displays lower peak displacements and stresses amplitudes than the composite deck counterpart and therefore could have been adopted as a

rational solution to the referred bridge's deck and may be employed in the design and worldwide rehabilitation of slender orthotropic steel bridge's decks.
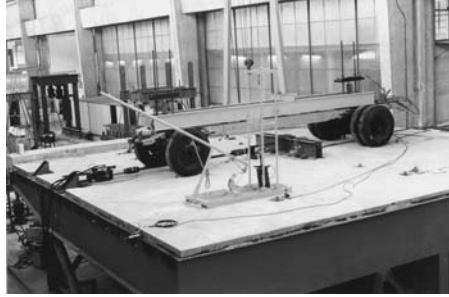
Figure 3: Upper view of the prototype scale model of the orthotropic deck at COPPE´s Laboratory of Structures; the deck already reinforced by a concrete slab on top of a visco-elastic layer.

2   ANALYTICAL – NUMERICAL MODEL FOR VEHICLE-BRIDGE INTERACTION

The equations of motion of the vehicle – bridge system were derived from equilibrium considerations applied to the free-body diagrams of the vehicle components and their connection to the bridge elements. Figure 4a shows the model of a 3 axles rigid vehicle traveling with constant velocity along the road surface of a bridge whose deck is represented by quadrilateral plane finite elements which combine flexural and membranes degrees of freedom. In this figure m_{pi} (i=1,6) correspond to the masses of the wheels – axle systems while m_v is the vehicle's body mass. In addition to the vertical displacement degree of freedom (DOF) assigned to each mass, rotation about the transverse axis (pitch) was provided to the vehicle's body mass, totalizing 8 DOF. All the springs and dampers are assumed to behave linearly. For a multi-leaf spring suspension type, each spring stiffness k_{vi} is to be obtained from the typical non-linear load x deflection behaviour [8] as an average values in the range of the corresponding wheel load.

The equations of motion of the vehicle-bridge system in matrix form are given by

$$\mathbf{M\ddot{U}} + \mathbf{C\dot{U}} + \mathbf{KU} = \mathbf{F} \tag{1}$$

where $\mathbf{U}$ consists of the nodal displacement sub-vector $\mathbf{U}_e$ and the vehicle degrees of freedom; $\boldsymbol{M}$, $\boldsymbol{C}$ and $\boldsymbol{K}$ are respectively the mass, damping and stiffness matrices which include both bridge and vehicle characteristics and $\mathbf{F}$ is the nodal force vector. The damping matrix was considered proportional to mass and stiffness matrices (Rayleigh damping).

The interaction force on the ith contact point between the bridge and the vehicle is written as:

$$F_i(x,t) = f_{epi} + f_{api} \tag{2}$$

where f_{epi} and f_{api} are respectively the elastic and damping forces, which depend on the relative motion of the corresponding mass m_{pi} to the bridge contact point. The relative displacement is given by:

$$u_{pi} - (u_{ri} + U_{ei}) \tag{3}$$

where u_{pi} is the ith wheel vertical displacement, u_{ri} is the road surface roughness under the ith wheel and U_{ei} is the bridge vertical displacement at the instantaneous point of contact to this wheel. The force at each contact point i (eq.2) is then rewritten as:

$$F_i(x,t) = k_{pi}\left(u_{pi} - (u_{ri} + U_{ei})\right) + c_{pi}\left(\dot{u}_{pi} - (\dot{u}_{ri} + \dot{U}_{ei})\right) \tag{4}$$

where k_{pi} and c_{pi} are the stiffness and damping coefficients of the ith axle-wheel system, $\dot{u}_{pi}$ and $\dot{U}_{ei}$ are the vertical velocities of the mass m_{pi} and the bridge contact point respectively, $\dot{u}_{ri} = (du_{ri}/dx)V(t)$ and $V(t)$ is the vehicle velocity.

Applying each contact force (eq.4) to the nodal force vector, the equation of motion corresponding to U_{ei} can be expressed as follows (displaying only the diagonal terms):

$$m_e\ddot{U}_{ei} + \ldots + (c_e + c_{pi})\dot{U}_{ei} + \ldots + (k_e + k_{pi})U_{ei} + \ldots - c_{pi}\dot{u}_{pi} - k_{pi}u_{pi} = -(m_v g + m_{pi}g) - c_{pi}\dot{u}_{ir} - k_{pi}u_{ir} \ (5)$$

where m_e, c_e, k_e are respectively the mass, damping and stiffness coefficients corresponding to the structure. The coefficient matrices in eq. 1 change according to the vehicle position.

The coupled equations of motion of the vehicle and the bridge were solved in time domain by direct integration using Newmark scheme.

At the present stage the model considers that each interaction force (eq. 4) is uniformly distributed among the 4 nodal points of the shell element within which the point of contact is located (see Figure 3b).

The bridge surface profile was generated by applying the inverse discrete Fourier transform to a roughness spectrum as described by Honda *et al* [9]. The surface profile was assumed to be constant across the deck width. To take into account the tyres contact area, the value of u_{ri} in eq (2) is made equal to the average profile amplitude within the contact area, thus smoothing the original road profile.

(a)   (b)
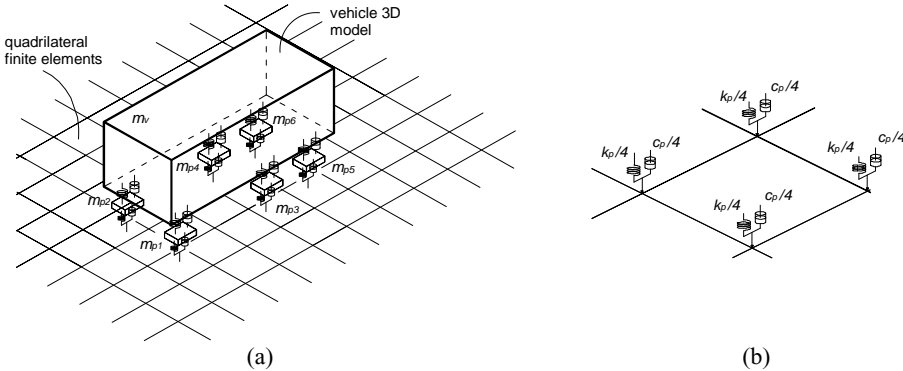
Figure 4: (a) Modeling of a 3 axles rigid vehicle traveling on a bridge deck modeled by quadrilateral plane finite shell elements; (b) detail of the contact points.

3 MODELING OF VISCO-ELASTIC MATERIALS

The visco-elastic layer in the sandwich solution was modeled by linear hexahedral elements shown in Figure 5, with 8 physical nodes and one fictitious node (dissipation node). The analytical model of the visco-elastic material follows the Golla Hughes Method (GHM) [10]. This method was proposed to circumvent the problem of frequency dependent properties of the visco-elastic materials in a time domain analysis. It consists in obtaining an equivalent dynamic system expressed in time domain involving visco-elastic materials modeled in Laplace domain. In this equivalent system additional degrees of freedom, called dissipation degrees of freedom are added to the mass, damping and stiffness matrices.

An important step in the GHM is the selection of the dissipation function $h(s)$ and therefore the approximation of the complex modulus on Laplace domain. For the computational tool specially developed to deal with these materials [5,6] the dissipation function proposed by Biot [11] was used with two terms in the series resulting in the following expression:

$$h(s) = \frac{\alpha s^2 + \gamma s}{s^2 + \beta s + \delta} \tag{6}$$

where $(\alpha,\beta,\delta,\gamma) > 0$. These parameters are selected in order to represent the variation with frequency of the modulus of elasticity and the loss factor of the visco-elastic material (VEM).
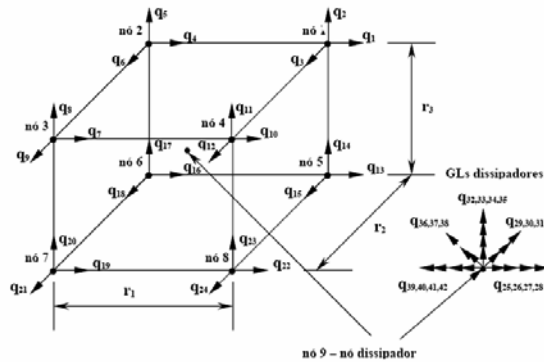
Figure 5: Linear hexahedral element with nodes and additional (dissipation) degrees of freedom for a VEM.

4 MODEL OF THE ORTHOTROPIC STEEL DECK

Figures 6 show the finite element model (FEM) of half cross section (see Fig.1a) of the actual steel orthotropic deck with three longitudinally stiffened panels spanning on four transverse floor-beams. Four node shell elements that combine separate membrane and plate bending behaviors were selected to model the deck plate, the trapezoidal stiffeners and the floor-beams' webs while the lower flange of the floor-beam and the central and lateral reinforced concrete barriers were represented by spatial frame elements. This model was initially calibrated in terms of experimental natural frequencies and associated vibration modes obtained from in *situ* measurements [1,2].

To model the concrete layer and the stud connectors in the actual composite deck (Figure 2b), shell elements and spatial frame elements were respectively added to the model of Fig.6. The shear connectors were considered embedded in the concrete layer and therefore, restrained to deform by bending and shear. The shell elements representing the concrete layer were disposed at its midplan and connected to the shell elements representing the steel plate by the stud elements and also by axially rigid elements to prevent the interpenetration of the concrete and steel layers. This second model was also calibrated in terms of experimental natural frequencies and vibration modes obtained from the 2002 measurements campaign [4].

The sandwich solution model (Figure 2a) was developed by adding to the steel deck model (Figs. 6) hexahedral elements to represent the 5 mm thick visco-elastic layer and on its top shell elements to simulate the reinforced concrete slab. Table 1 presents a comparison between the theoretical vibration frequencies resulting from the numerical model and those obtained from experimental free vibration tests on the prototype scaled model of the sandwich deck shown in Figure 3. The description of the vibration mode shapes associated to these frequencies is also given in this table. Non-conformities between the bearing conditions of the prototype scale model and the boundary conditions simulated by the numerical FEM model are the main cause for the small differences between theoretical and experimental frequency values shown in Table 1.

(a)

(b)
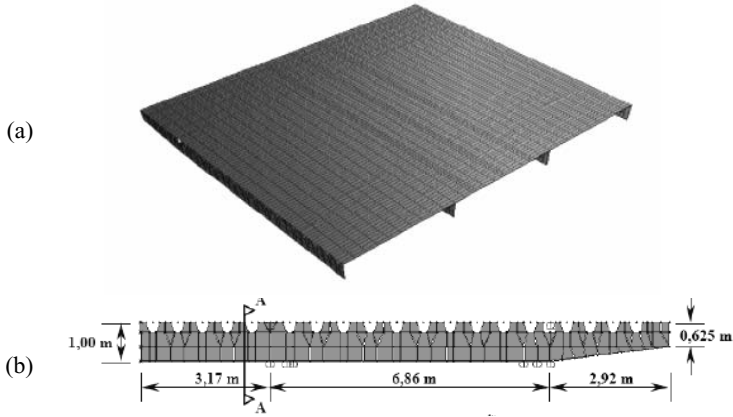
Figures 6: (a) FEM model of the three spans stretch of the orthotropic deck; (b) half deck cross section of the model showing a floor-beam.

Figures 7 illustrate two vibration bending modes of the deck: one of the cantilevered deck panels (Fig.7a) and the other of the deck panels between webs of the box girders (Fig. 7b). In both alternative deck solutions, these modes appear associated to frequencies close to each other as given in Figure 7; the composite deck displaying the higher frequencies and thus the greater stiffness.

Table 1: Natural frequencies and vibration modes of the sandwich deck

Experimental (Hz ± 0.4Hz)	Numerical (Hz)	Mode shape
	12.6	Bending of cantilevered deck panel
14.4		Bending of cantilevered deck panel
	15.7	
24.8		
	25.0	Bending of deck between girder webs
	25.8	Bending of deck between girder webs
	27.8	Bending of deck between girder webs
	27.9	Bending of deck between girder webs
30.3		
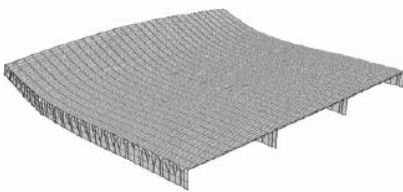
(a) f= 12.6 Hz for the sandwich deck
f = 13.3 Hz for the composite deck
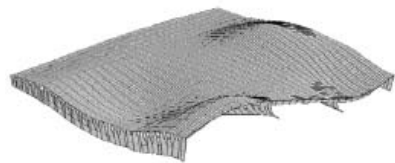
(b) f=27.9 Hz for the sandwich deck
f = 29.5 Hz for the composite deck

Figures 7: Typical free vibration modes of the deck. (a) bending of the cantilevered deck panels. (b) bending of deck panels between webs of the box girders.

5 DYNAMIC DECK RESPONSES

5.1 Responses to impact loads

The structural performance of each of the two alternative solutions was first evaluated for an impact load function which consists of a series of triangular impulsive loads applied at 3.0 s time interval. This simplified load function was applied as preliminary approach to the effect of wheel loads produced by multi-axles truck passing on poorly maintained expansion joints. The time and frequency responses in terms of vertical displacement at the edge of the floor-beam cantilever due to the impact loads applied at midspan between webs of the box girder are shown respectively in Figure 9a and in Figure 9b. In Fig. 9a it can be seen that the sandwich deck displays lower amplitudes than the composite deck, and greater damping. These lower amplitudes occur for all excited modes as can be observed in Fig.9b.

(a)   (b)
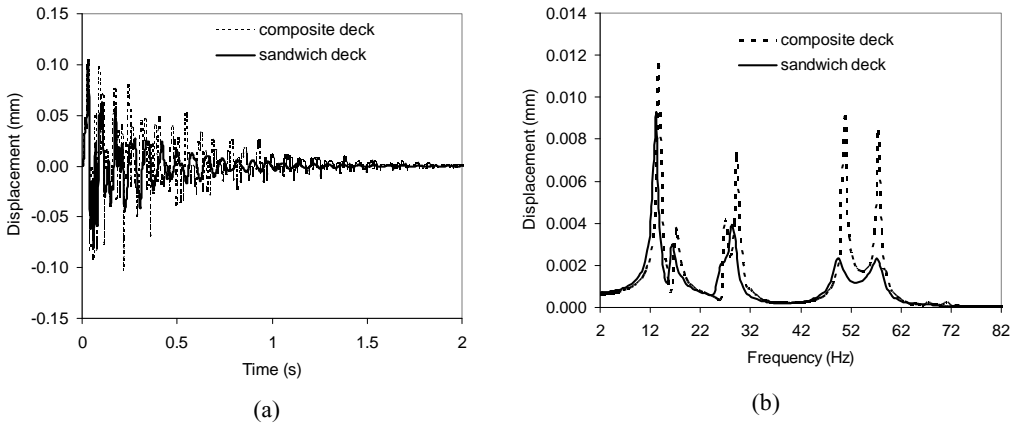
Figures 9: Vertical displacement responses at the edge of the floor-beam cantilever due to impact loads applied at midspan between box girder webs. (a) time domain; (b) frequency domain.

5.2 Responses to the passage of a three-axles truck

(b)
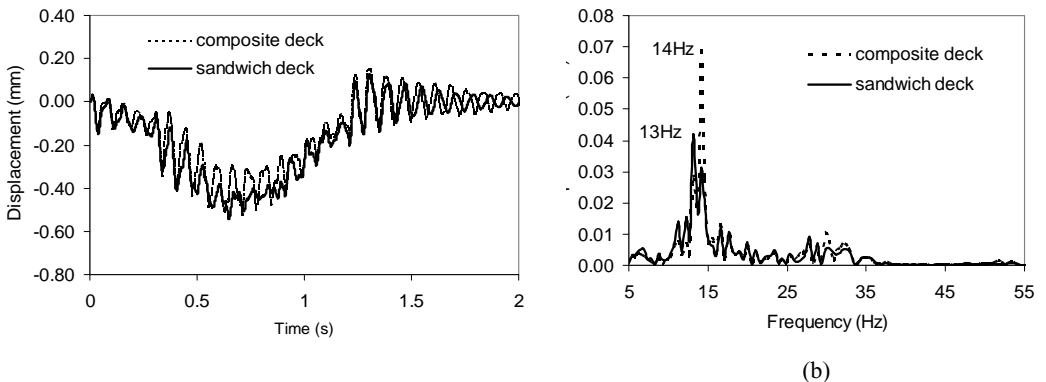
Figures 10. Vertical displacement responses at the edge of the cantilevered deck panel due to the three axles truck traveling along the slow lane with constant velocity equal to 60 km/h. (a) time domain; (b) frequency domain.

With the analytical-numerical model for vehicle-structure interaction described in section 2 the two orthotropic deck alternative solutions were subjected to the passage of a 3 axles truck weighing 215 kN with constant velocity. In the structural analysis the concrete pavement was considered in bad condition.

The time and frequency responses in terms of vertical displacement at the tip of the cantilevered deck panel between two floor-beams due to the passage of the truck along the slow lane are shown respectively in Figure 10a and in Figure 10b. It is shown that the sandwich solution displays lower peak displacement amplitudes than the composite deck. These peak amplitudes are associated to the bending vibration mode involving the cantilevered deck panel (Fig. 7a).

6   CONCLUSIONS

The performance of two alternative solutions devised to enhance the structural dynamic behaviour and fatigue life of slender and lightweight orthotropic steel deck are investigated by means of a specially developed numerical model which includes layers of visco-elastic materials. An experimentally calibrated numerical model of an existing orthotropic deck is used for this purpose and the obtained results have shown that the sandwich deck displays lower peak displacements and stresses amplitudes than the composite deck counterpart and therefore can be adopted as a rational solution in the design of new bridges and also be employed in the rehabilitation of slender orthotropic decks of existing steel bridges.

REFERENCES

[1]   Battista R.C., Pfeil M.S., Roitman N., Magluta C., " Global analysis of the structural behaviour of the central spans of Rio-Niterói Bridge", *PONTE SA Concessionaire of Rio Niterói Bridge – Contract Report COPPETEC ET150747*, Rio de Janeiro, 1997 (in Portuguese).

[2]   Battista, R.C., Pfeil, M. S. "Strengthening fatigue-cracked steel bridge decks. *Proceedings of the Institution of Civil Engineers,* 157, 93 - 102, 2004.

[3]   Battista R.C., BatistaE.M., Pfeil M.S., "Experimental tests on a prototype scale model of the slender steel orthotropic deck of Rio-Niteroi bridge ", *Ponte SA -Concessionaire of the Rio-Niteroi Bridge-Contract report COPPETEC ET-150771*, Rio de Janeiro, Brasil (in Portuguese), 1998.

[4]   Battista, R.C., Pfeil, M.S., Carvalho, E.M.L., "Fatigue life estimates for a slender orthotropic steel deck", *Journal of Constructional Steel Research*, **64**(2), 134- , 2008.

[5]   Barbosa F.S., "Computational modeling of structures with viscoelastic damping layers", D.Sc. thesis, COPPE – UFRJ, Rio de Janeiro, 2000 (in Portuguese).

[6]   Vasconcelos, R.P., "Vibration dynamic control by viscoelastic devices", D.Sc. thesis, COPPE – UFRJ, Rio de Janeiro, 2003 (in Portuguese).

[7]   Santos, E.F., "Analysis and mitigation of vibration in motorway bridges", D.Sc. thesis, COPPE – UFRJ, Rio de Janeiro, 2007 (in Portuguese).

[8]   Gillepsie T.D., Karamihas S.M., Cebon D. et al, "Effects of heavy vehicle characteristics on pavement response and performance", The University of Michigan Transportation Research Institute, UMTRI92-2, 1992.

[9]   Honda, H., Kajikawa, Y., Kobori, T., Spectra of Road Surface Roughness on Bridges. *J. Struct. Div. ASCE*, vol. 108, ST9, pp1956-66, 1982.

[10] Golla, D.F.; Hughes, .C.; "Dynamics of viscoelastic Structure", *Journal of Applied Mechanics*, 52, 897-906, 1985 .

[11] Biot M.A., "Variational Principles in irreversible thermodynamics with applications to viscoelasticity", Physical Review, vol. 97 n. 6, pp 1463-1469, 1955.